Coherence resonances and band gaps in plasmonic hole arrays

Matt Smith and Greg Gbur

Phys. Rev. A **99**, 023812 — Published 6 February 2019

DOI: 10.1103/PhysRevA.99.023812

Coherence Resonances and Bandgaps in Plasmonic Hole Arrays

Matt Smith* and Greg Gbur†
The University of North Carolina at Charlotte
(Dated: January 9, 2019)

We demonstrate theoretically the existence of optical coherence bandgaps by performing simulations of partially coherent light incident on a linear array of circular holes in a subwavelength-thickness gold sheet. We use a simple scalar Foldy-Lax system of equations for our model. A possible physical mechanism for the bandgaps is discussed.

I. INTRODUCTION

The coherence of a light field can affect many of the observable characteristics of the field as it propagates, including its directionality [1], its spectrum [2], and its state of polarization [3, 4]. Consequently, the ability to control spatial coherence allows control over the properties of a field as it propagates. Furthermore, it is known that partially coherent light is beneficial in a number of applications, such as free-space optical communications [5, 6], and that the degree of coherence must be optimized for the specifics of the communications channel. The ability to control spatial coherence is therefore of great importance.

It has been shown theoretically that the spatial coherence of light can be modulated in a Young double-slit experiment in which the slits are in a surface plasmon-supporting metal, and that the coherence can be increased or decreased with the appropriate geometry [7]. Some of these predictions were confirmed experimentally [8–10]. It was further shown that adding a third slit to the plasmon-supporting material can further modulate coherence, and that the middle slit does not act as a significant barrier to plasmon coupling between the outer two [11]. Based on this, an array of holes in a metal plate was proposed as a coherence-converting plasmonic device [12]. In the simulations undertaken, however, the hole arrays almost universally caused an increase in the spatial coherence, and no significant decreases.

In this work, we study computationally the spatial coherence of light transmitted through a plasmon-supporting metal plate possessing a one-dimensional array of holes. We demonstrate that such arrays produce extended spectral regions in which plasmon coherence effects are significantly suppressed. These regions represent a previously unrecognized phenomenon that we refer to as spatial coherence bandgaps.

II. DESCRIPTION OF MODEL

We use the scalar cylindrical wave model of Ref. [12] to describe the effects of plasmonic scattering; here we review the salient details. Figure 1 illustrates the process for a 1×3 array of holes of radius a separated with period d. A quasi-monochromatic input field with central wavelength λ_0 illuminates the plate from the $z < 0$ side; at each hole, part of the illuminating field is directly transmitted, and part of it is coupled into a cylindrical surface plasmon wave. When the plasmon wave interacts with another hole, it can couple back into a propagating light wave, where it can interfere with the directly transmitted wave. If the fields illuminating each of the holes are mutually incoherent, the light emanating from the holes will in general be a mixture of all three inputs; the light coming out of the holes is therefore partially coherent.

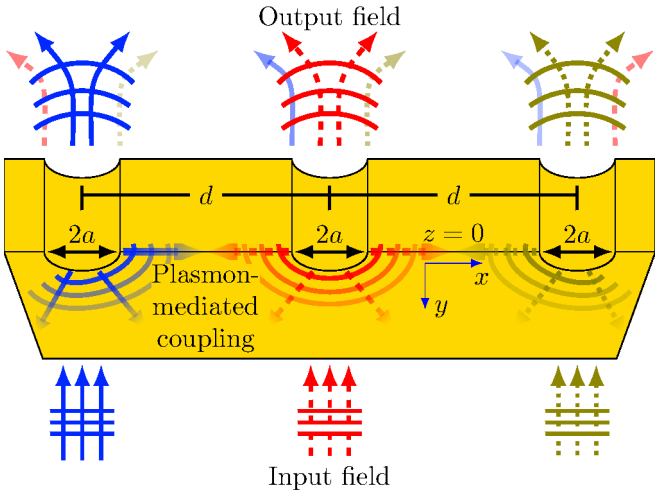

FIG. 1. A cut-away sketch of a 1×3 plasmonic hole array, viewed from the $z < 0$ side of the plate, showing the coherence conversion process. (Note that the input field is the same everywhere in the plane; the arrows in the figure are color-coded only to indicate which hole they are incident upon.)

To model this process, we first consider a coherent input field $\phi_k(x)$, where k represents a variable parameter of the field, incident upon a row of holes lying along the x axis. We take the field to be polarized along the x axis, so we may use a scalar field. Upon striking a hole at location x_n, some fraction α of the mode will transmit directly through the hole, and some fraction will couple to the plate as a surface plasmon wave and propagate

* msmit473@uncc.edu
† gjgbur@uncc.edu

to other holes. Assuming that the holes have subwavelength diameter and that the distance between the holes is larger than the wavelength, the holes may be treated as point scatterers. The output field at location x_n is thus

$$\psi_k(x_n) = \alpha\phi_k(x_n) + \beta \sum_{m=1,m\neq n}^{N} G(x_n, x_m)\psi_k(x_m). \quad (1)$$

where N is the number of holes in the array and $G(x_n, x_m)$ is a cylindrical wave that has propagated from x_m to x_n and represents the scattered surface plasmon. The cylindrical wave may be written as

$$G(x_n, x_m) = \frac{\mathrm{i}}{4} H_0^{(1)}\left(k_{\mathrm{sp}}\left|x_n - x_m\right|\right), \quad (2)$$

where $H_0^{(1)}$ is the zeroth-order Hankel function of the first kind, k_{sp} is the surface plasmon wavenumber,

$$k_{\mathrm{sp}} = k_0\sqrt{\frac{\epsilon_0\epsilon_m}{\epsilon_0 + \epsilon_m}}, \quad (3)$$

ϵ_m is the dielectric constant of the metal, ϵ_0 is the dielectric constant of free-space, and $k_0 = 2\pi/\lambda_0$ is the free-space wavenumber. We model ϵ_m as a function of λ_0 using a critical points model [13, 14]. The scattering parameter β is estimated by treating a cylindrical hole as a spherical cavity in a solid metal background; the details can be found in Ref. [12]. The result is that β may be written as

$$|\beta| \approx \left(\frac{2\pi a}{\lambda_0}\right)^3 \left|\frac{(1 - \epsilon_m/\epsilon_0)}{(1 + 2\epsilon_m/\epsilon_0)}\right|. \quad (4)$$

Equation (1) represents a Foldy-Lax system of N equations with N unknowns which can be solved using matrix methods; the solution results in the value of $\psi_k(x)$ at the output of each hole.

So far, we have considered only spatially coherent fields propagating through the system. Partial coherence is characterized by use of the cross-spectral density $W(x_n, x_m)$,

$$W(x_n, x_m) = \left\langle U^*(x_n)U(x_m)\right\rangle_\omega, \quad (5)$$

where the average is over an ensemble of monochromatic fields $U(x)$ of frequency ω [15]. In general, the cross-spectral density may be written in terms of the spectral density $S(x)$ at each hole and the spectral degree of coherence $\mu(x_n, x_m)$ between holes as

$$W\left(x_n, x_m\right) = \sqrt{S\left(x_n\right)S\left(x_m\right)}\mu\left(x_n, x_m\right). \quad (6)$$

The spectral degree of coherence is a normalized quantity that represents the strength of correlations between two points in the field, with $|\mu| = 1$ representing complete coherence, and $|\mu| = 0$ representing incoherence.

We consider the special case of an incident field which has a uniform spectral density across the $z = 0$ plane and has degree of coherence μ_0 of Gaussian Schell-model form, i.e.

$$\mu_0\left(|x_m - x_m|\right) = \exp\left(\frac{-\left|x_m - x_n\right|^2}{2\delta^2}\right), \quad (7)$$

where δ is the transverse correlation length.

To propagate this partially coherent field through the hole array, we first write μ_0 in terms of its spatial Fourier transform,

$$\mu_0(|x_m - x_n|) = \int_{-\infty}^{\infty} \tilde{\mu}_0\left(k\right)\mathrm{e}^{\mathrm{i}k(x_m - x_n)}\mathrm{d}k, \quad (8)$$

where

$$\tilde{\mu}_0\left(k\right) = \frac{\delta}{\sqrt{2\pi}}\exp\left(-\frac{1}{2}\delta^2k^2\right). \quad (9)$$

It then follows, using Eqs. (6) to (9), that the cross-spectral density of the input field may be written as an incoherent superposition of coherent modes as

$$W_0(x_n, x_m) = \int_{-\infty}^{\infty} \tilde{\mu}_0\left(k\right)\phi_k^*(x_n)\phi_k(x_m)\mathrm{d}k, \quad (10)$$

where

$$\phi_k(x) = \sqrt{S_0}\mathrm{e}^{\mathrm{i}kx}. \quad (11)$$

and we have assumed a uniform spectral density S_0 across the entire input plane. We see now that k represents a transverse wavenumber.

As the modes $\phi_k(x)$ propagate through the plasmonic system, they will remain mutually incoherent, and the weighting factor $\tilde{\mu}_0\left(k\right)$ will remain unchanged. The cross-spectral density of the output field will therefore be

$$W_f(x_n, x_m) = \int_{-\infty}^{\infty} \tilde{\mu}_0\left(k\right)\psi_k^*(x_n)\psi_k(x_m)\mathrm{d}k, \quad (12)$$

where $\psi_k(x)$ is determined by numerically solving Eq. (1). We may therefore evaluate $W_f\left(x_n, x_m\right)$ by propagating individual modes $\phi_k(x)$ through the system and combining them together using Eq. (12). With this result, the output spectral degree of coherence $\mu_f\left(x_n, x_m\right)$ can be calculated.

III. RESULTS AND DISCUSSION

There is one significant difficulty in studying the coherence of the field output by the plasmonic hole array. Though the input field is Schell-model, and the overall degree of coherence can be characterized by the single parameter δ, the output field is no longer Schell-model, and the degree of coherence will generally be different for light being emitted from any pair of holes. To talk about overall changes to the spatial coherence of the output

field, we need to define a single number that accurately characterizes this global coherence.

We therefore define the average output coherence of the array M_f by the following formula:

$$M_f = \frac{1}{N}\sum_{n=1}^{N}\frac{1}{N-1}\sum_{m=1,m\neq n}^{N}\left|\mu_f\left(x_n, x_m\right)\right|. \tag{13}$$

The average input coherence M_0 is defined similarly in terms of $\mu_0\left(x_n, x_m\right)$. This expression is the average of the spectral degree of coherence, taken over all pairs of holes. It is to be noted that the absolute value of the degree of coherence is used in the expression, to avoid spurious low values that could come from different terms being out of phase. It should also be noted that the magnitude of this quantity will generally decrease as the array size is increased, as the coherence of more distant pairs of holes will be included.

In our simulation code, we arbitrarily decided to set α to 0.5; however, we note that for our calculations it makes no difference what the value of α is, as long as it is nonzero, since it is present in both the numerator and denominator of $\mu\left(x_n, x_m\right)$ in such a way that it is canceled out.

In Fig. 2, we plot M_f and M_0 as a function of λ_0 for several array sizes from 1×2 to 1×100, with d and δ both set to 1000 nm. As the array goes from 1×2 to 1×5, the broad peak on the left narrows, while M_f elsewhere flattens to around the same value as M_0. At the 1×10 array, a new peak emerges at around 710 nm, which redshifts and splits into multiple peaks as the array size increases. Just to the left of this peak (or series of peaks) is a region between $\lambda_0 \approx 670$ nm and $\lambda_0 \approx 700$ nm where M_f is flat and roughly equal to M_0. This flat region exhibits a dependence on the number of holes analogous to the dependence that a transmittance bandgap has on the number of layers in a photonic crystal. This suggests that this flat region is a bandgap, but one which affects optical coherence rather than optical intensity.

If this flat region is truly a bandgap, it should be sensitive to the periodicity of the array; if the periodicity of the array is destroyed, the flat region should be destroyed. We test this sensitivity by randomizing the hole positions within the array to destroy the periodicity and observe how the coherence changes. The randomization procedure is as follows. A given hole, say, hole n, has non-randomized location x_n. We obtain the randomized location X_n via

$$X_n = x_n + Z_n\sigma, \tag{14}$$

where Z_n is a number drawn from the standard normal distribution and σ is a chosen standard deviation. We constrain the randomized location such that for every hole pair, say, X_n and X_m, we have $|X_n - X_m| > 2a$. This is to prevent the holes from overlapping. If any holes did not satisfy this condition, we discarded that sample configuration and obtained a new one until the condition was met. Figure 3 shows randomization results for a 1×20 array with d and δ set to 1000 nm, with $\sigma = 50$ nm, 75 nm, and 100 nm. For each value of σ, M_f was calculated for 100 configurations, and the average of those M_f is shown in Fig. 3. The unrandomized case ($\sigma = 0$ nm) is also shown. We can see that as σ increases, the prominent peaks at $\lambda_0 \approx 550$ nm and $\lambda_0 \approx 715$ nm gradually disappear and the flat region located at $\lambda_0 \approx 690$ nm disappears as the coherence becomes basically a single broad peak. This indicates that the flat region is a bandgap.

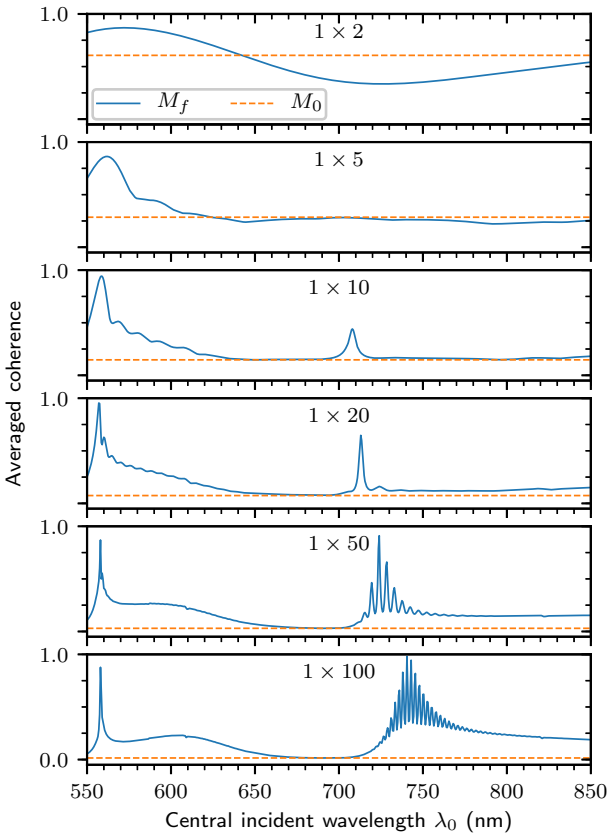

FIG. 2. Averaged output and input coherence for increasingly large hole arrays, with $d = 1000$ nm and $\delta = 1000$ nm. There is a flat dip between $\lambda_0 \approx 660$ nm and $\lambda_0 \approx 700$ nm; this is the coherence bandgap we will be examining. It is noticeable with as few as 10 holes in the array.

Having established the existence of coherence bandgaps, we now need to understand their cause. To do this, consider the plasmon waves between a pair of holes at locations x_1 and x_2, as depicted in Fig. 4. Confining our attention to x_1 for the moment, we consider three plasmon waves: the plasmon wave denoted G_1 propagating from x_1 to x_2, a reflected wave G_{1r}, and a wave G_2 propagating from x_2 to x_1. The argument of G_2 will be $\mathcal{R}\{k_{\mathrm{sp}}\}\,d$ at x_1, where $\mathcal{R}\{\}$ denotes the real

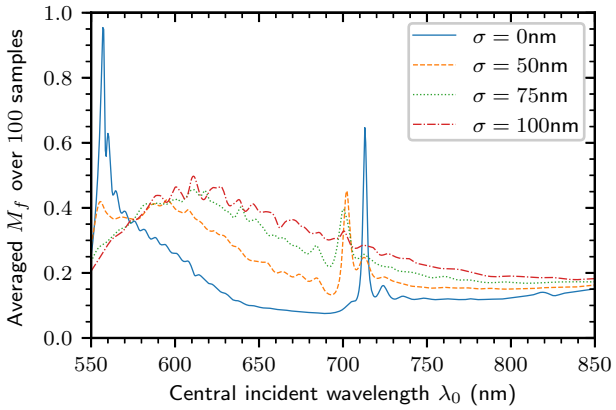

FIG. 3. Coherence of randomized 1×20 hole arrays, with $d = 1000\,\text{nm}$ and $\delta = 1000\,\text{nm}$. For each value of σ (except 0), 100 randomizations were done, and their averaged coherence M_f calculated. These M_f were then averaged together to produce this figure.

part. When the argument of G_2 is

$$\mathcal{R}\{k_{\text{sp}}\}\, d = \nu_2 \pi, \tag{15}$$

where ν_2 is an integer, then G_2 will have constructive (destructive) interference with G_1 when ν_2 is even (odd). We call these "ν_2 modes." Similarly, the argument of G_{1r} will be $\mathcal{R}\{k_{\text{sp}}\}\, 2d$ and will have constructive (destructive) interference with G_1 when

$$\mathcal{R}\{k_{\text{sp}}\}\, 2d = \nu_{1r} \pi, \tag{16}$$

where ν_{1r} is again an even (odd) integer. We call these "ν_{1r} modes." Combining Eqs. (15) and (16), we can see that at any value of $k_{\text{sp}}d$ where these conditions coincide, ν_2 and ν_{1r} have the relationship

$$\nu_{1r} = 2\nu_2. \tag{17}$$

At x_2, there are identical relationships between G_2, G_1, and a reflected G_2 wave. Furthermore, in an arbitrarily-sized array, every hole will have these relationships with its neighboring holes, all at the same wavelength. Thus, the entire array will obey the relationships in Eqs. (15) to (17), meaning that the entire array will have identical ν_2 modes and identical ν_{1r} modes.

If we consider this behavior as a function of $\mathcal{R}\{k_{\text{sp}}\}\, d$, this means that ν_2 modes will only ever coincide with constructively interfering ν_{1r} modes, that there will be a destructive ν_{1r} mode between these combined modes, and that these combined modes will alternate between constructive and destructive ν_2 modes. This behavior will be demonstrated in Fig. 5.

Figure 5 shows the averaged coherence of a 1×50 array as a function of $\mathcal{R}\{k_{\text{sp}}\}\, d$. The ν_2 and ν_{1r} modes are indicated. In order to show many cycles, in Fig. 5 we have neglected the wavelength dependence of ϵ_m and

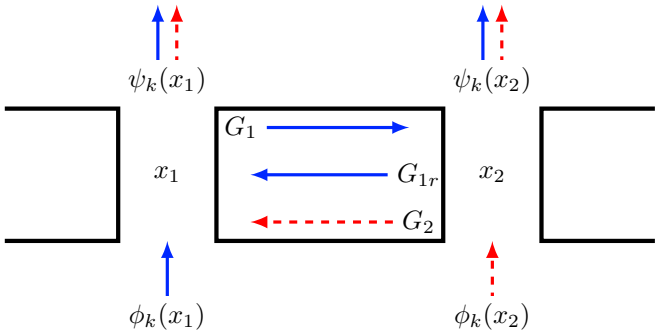

FIG. 4. Notation for plasmonic interference between two holes.

β. Looking at Fig. 5, we can make a few observations. First, we can note that that coherence peaks occur near multiples of π, and that when ν_2 is even, we tend to have higher peaks than when it is odd. This is because at these wavelengths with even ν_2, both G_2 and G_{1r} are in phase with G_1, which increases the coherence. Second, we can note that the flat bandgaps occur near peaks at odd values of ν_2. This is because around these wavelengths, particularly in the region between here and where ν_{1r} is also odd, G_2 and G_{1r} will destructively interfere with G_1. This minimizes the plasmonic contribution to the overall field, which reduces the output coherence to near its input value. This is the mechanism behind the bandgap regions. It should be noted that in our testing there are not *always* bandgaps at odd ν_2, but they do appear *only* at odd ν_2.

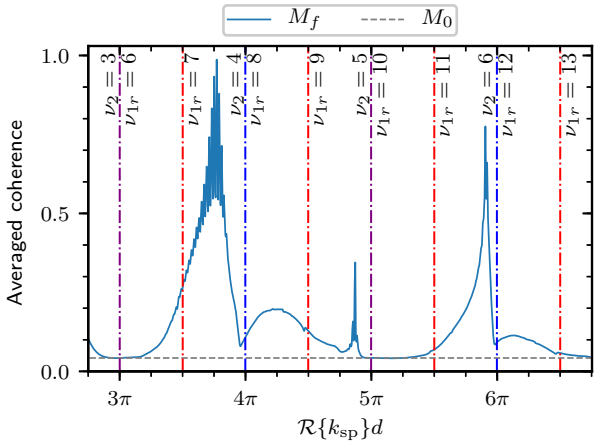

FIG. 5. M_f for a 1×50 array, with $d = 1200\,\text{nm}$ and $\delta = 1500\,\text{nm}$. Here, the dielectric constant and scattering parameter were set to constant values of $\epsilon_m \approx -10.6488{+}\text{i}1.3734$ and $\beta = 5$, independent of wavelength. Red lines are wavelengths of destructive interference, blue of constructive interference, and purple is where the two coincide.

The coherence peaks observed in these simulations may also be interpreted in another way: as a classical form

of superradiance and subradiance. Quantum superradiance, first introduced by Dicke [16], is a phenomenon in which closely-packed atoms end up radiating coherently due to their interaction with a mutual radiation field. For our purposes, we may imagine this as each atom having two contributions to its radiation: direct spontaneous emission, and emission stimulated by constructive radiation from the other atoms. Subradiance, in contrast, is the result of destructive interference suppressing the radiation rate. In a plasmonic hole array, superradiance and subradiance may be interpreted as arising from the interactions between the directly transmitted light at each hole and the plasmonic contribution, as first discussed by Ropers et al. [17].

Referring back to Fig. 2, the coherence peak at 750 nm is evidently the subradiant peak, while the coherence peak at 560 nm is the superradiant peak. This can be partly justified by looking at the two-hole case at the top of the figure, in which the coherence is near maximum at around 550 nm, and near minimum at around 750 nm; these are regions in which the coherent part of the transmitted field is enhanced and suppressed, respectively, due to the interaction between the holes. In contrast to Ref. [17], however, the peaks observed here are peaks in the spatial coherence of the transmitted light, not in the intensity of the transmitted light itself.

It is to be noted that connections between surface plasmons and spatial coherence have been considered elsewhere in recent years, albeit in a very different context. Friberg et al. [18–20] have considered the control and modification of the spatial coherence of surface plasmons themselves, without their effect on transmitted light. Their results indicate that there is much more to be studied in partially coherent surface plasmon optics.

IV. SUMMARY

In summary, we have theoretically demonstrated the existence of optical coherence bandgaps caused by surface plasmons in linear arrays of circular holes in a thin metal sheet. We have also proposed a physical mechanism causing these bandgaps. It is important to note that the bandgaps discussed here are not of the typical form, which result from the interference of waves along the longitudinal direction of propagation. Here, it is the transverse coherence properties of the field that are suppressed through the interactions of propagating plasmons. The observed effects appears to be a bandgap phenomenon that has previously gone unobserved.

ACKNOWLEDGMENTS

This research is supported by the U.S. Air Force Office of Scientific Research (USAFOSR) under Grant FA9550-16-1-0240.

We would like to thank a referee for noting the relationship of our results to superradiance and subradiance.

[1] E. Wolf, J. Opt. Soc. Am. **68**, 6 (1978).
[2] E. Wolf and D. F. V. James, Rep. Prog. Phys **59**, 771 (1996).
[3] D. F. V. James, J. Opt. Soc. Am. A **11**, 1641 (1994).
[4] E. Wolf, Opt. Lett. **28**, 1078 (2003).
[5] G. Gbur and O. Korotkova, J. Opt. Soc. Am. A **24**, 745 (2007).
[6] A. Dogariu and S. Amarande, Opt. Lett. **28**, 10 (2003).
[7] C. H. Gan, G. Gbur, and T. D. Visser, Phys. Rev. Lett. **98**, 043908 (2007).
[8] N. Kuzmin, G. W. 't Hooft, E. R. Eliel, G. Gbur, H. F. Schouten, and T. D. Visser, Opt. Lett. **32**, 445 (2007).
[9] S. Divitt, M. Frimmer, T. D. Visser, and L. Novotny, Opt. Lett. **41**, 3094 (2016).
[10] D. Li and D. Pacifici, Sci. Adv. **3**, e1700133 (2017).
[11] C. H. Gan and G. Gbur, Plasmonics **3**, 111 (2008).
[12] C. H. Gan, Y. Gu, T. D. Visser, and G. Gbur, Plasmonics **7**, 313 (2012).
[13] P. G. Etchegoin, E. C. Le Ru, and M. Meyer, J. Chem. Phys. **125**, 164705 (2006).
[14] P. G. Etchegoin, E. C. Le Ru, and M. Meyer, J. Chem. Phys. **127**, 189901 (2007).
[15] E. Wolf, J. Opt. Soc. Am. **72**, 343 (1982).
[16] R. H. Dicke, Phys. Rev. **93**, 99 (1954).
[17] C. Ropers, D. J. Park, G. Stibenz, G. Steinmeyer, J. Kim, D. S. Kim, and C. Lienau, Phys. Rev. Lett. **94**, 113901 (2005).
[18] A. Norrman, S. A. Ponomarenko, and A. T. Friberg, Europhys. Lett. **116**, 64001 (2016).
[19] Y. Chen, A. Norrman, S. A. Ponomarenko, and A. T. Friberg, Opt. Lett. **42**, 3279 (2017).
[20] Y. Chen, A. Norrman, S. A. Ponomarenko, and A. T. Friberg, Opt. Lett. **43**, 3429 (2018).